

# Motion Generators of Quadrics-Circular, Cylindrical, and Conical Surfaces

Shuofei Yang, Yangmin Li\*

The Hong Kong Polytechnic University, Department of Industrial and Systems Engineering,  
Kowloon 999077, Hong Kong, China

**Abstract:** This paper presents research work on synthesis of the mechanical structures that generate translations on circular, cylindrical, and conical surfaces. As these three kinds of surfaces are all basic quadrics, the synthesized structures are called motion generators of quadrics. Firstly, the characteristics of these quadrics are analyzed, which will result in an easy way to express them. Secondly, the motion sets of one-degree-of-freedom (one-DoF) joints are described by finite screws, which can lead to a simple and non-redundant manner for motion description of mechanisms. Based upon this, the motion generators of circular, cylindrical, and conical surfaces are respectively synthesized, and all the serial kinematic chains that generate these quadrics are obtained. The results are verified through simulations in MATLAB® software. Finally, as an application of the motion generators of quadrics, closed-loop linkages constituted by the generators of circular and cylindrical surfaces with specific geometric conditions are synthesized, which purely generate one-DOF translations along ellipse curves. Some new serial kinematic chains and closed-loop linkages are invented in this paper. These new mechanisms have simple mechanical structures, and they have potential applications in design of robots used in machining and manufacturing of complex surfaces and curves.

**Keywords:** Mechanism synthesis, Kinematics, Finite screw, Closed-loop linkage

## 1. Introduction

Mechanism synthesis (type or structure synthesis) is the fundamental issue in the research of mechanisms and robotics. Inventing new mechanisms with new motion patterns is an important and challenging work in mechanism synthesis. Here, motion pattern indicates finite motion pattern (full-cycle motion pattern) [1-3]. It means that for the motions generated by a mechanism, the corresponding motion pattern contains not only the number and types (rotations and/or translations) of degree-of-freedom (DoFs), but also detailed characteristics of each DoF, regardless of the mechanism's dimensions.

Till now, many mechanisms, including serial kinematic chains (serial mechanisms) [4,5], parallel manipulators (parallel mechanisms) [6-8], and closed-loop linkages (closed-loop mechanisms) [9-11], with different motion patterns, have been investigated. Among them, some typical examples are: the one-DoF translational mechanisms along circles [12]; the one-DoF rotational mechanisms having Bennett motion pattern [13], or having Bricard pattern [14]; the three-DoF translational mechanisms [15,16]; the three-DoF rotational mechanisms [17]; the three-DoF one-translational and two-rotational mechanisms having Z3 pattern [18], having Exechon pattern [19], or having RPR-equivalent pattern [20]; the four-DoF three-translational and one-rotational mechanisms with fixed rotational direction [21], with bifurcate rotational direction [22], or with variable rotational direction [23]; and so on. However, to the knowledge of authors, motion patterns on complex surfaces or along complex curves have been reported seldom in the existing works. This paper is focused on this topic, and some new motion patterns will be presented, whose translational parts are on quadrics like cylindrical and conical surfaces. The mechanical structures that generate these motion patterns will be synthesized, which are called motion generators of quadrics.

Taking into account that the non-redundant finite screw in quasi-vector form [24-26] is simpler and more concise than the other mathematical tools in describing finite motions of mechanisms, and its counterpart named instantaneous screw has been widely used in the velocity [27,28], accuracy [29,30], dynamics [31-34], and stiffness [35-38] analysis of mechanisms, we use finite screw as a mathematical tool in synthesizing serial kinematic chains and closed-loop linkages in this paper.

Based upon the existing works, this paper studies the analytical expressions to describe translational motion patterns on circular, cylindrical, and conical surfaces as well as along ellipse curves. The synthesis of motion generators of these surfaces and curves is presented. The synthesized serial kinematic chains generate two-DoF translations on quadrics. And the synthesized closed-loop linkages purely generate one-DoF translations along ellipse curves. These mechanisms have potential applications in the innovative design of robots used in machining and manufacturing of complex surfaces and curves.

The outline of the paper is as follows: After conducting a brief review of the state-of-the-art of motion pattern description and mechanism synthesis in Section 1, we give an analysis of the characteristics of the three basic kinds of quadrics, and provide an easy way to express them in Section 2. In Section 3, the motion sets of simple joints and serial kinematic chains are described by finite screws, motion generators of circular, cylindrical, and conical surfaces are respectively synthesized, and their motion patterns are verified through simulations in MATLAB® software. Applying the motion generators of quadrics, closed-loop linkages with one-DoF translational motion pattern along ellipse curve are investigated in Section 4, before the conclusions drawn in Section 5. The research work presented in this paper lays solid foundation for synthesis of the motion generators of parabola curves and hyperbola curves.

---

\* Corresponding Author: yangmin.li@polyu.edu.hk

## 2. Three basic kinds of quadrics

Quadrics are the two-dimensional surfaces whose expressions contain two independent parameters. In this paper, we focus on the three basic kinds of quadrics. They are circular surface, cylindrical surface, and conical surface. The coordinates of any point on one of these three kinds of surfaces can be expressed by polar coordinates, which consist of a length and an angle.

As shown in Fig. 1, a circular surface is a plane in shape of disc with given radius. On this surface, any point  $A$  is identified by a vector  $\mathbf{r}$  pointing from the disc center  $O$  to the point. The point coordinates are expressed by the vector length  $t$ , and the angle  $\theta$  between the vector and a referenced direction  $s_x$ .

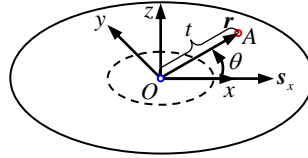


**Fig. 1** A circular surface.

A cylindrical surface with given radius and height is shown in Fig. 2. For any point  $A$  on this surface, a vector  $\mathbf{r}$  pointing from the center  $O$  of the cylinder bottom to that point is used to identify the point. The point coordinates are expressed by the length  $t$  of the vector projection along the cylinder generatrix, and the angle  $\theta$  between the vector projection on the bottom and a referenced direction  $s_x$ .

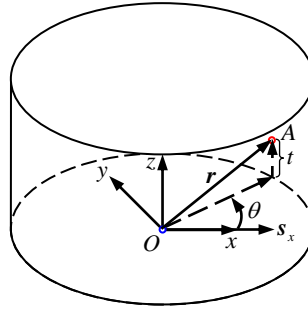


**Fig. 2** A cylindrical surface.

Similarly, for any point  $A$  on a conical surface with given radius and height, as shown in Fig. 3, a vector  $\mathbf{r}$  pointing from the center  $O$  of the conic bottom to that point is used to identify the point. The point coordinates are expressed by the length  $t$  of the vector projection along the conic generatrix, and the angle  $\theta$  between the vector projection on the bottom and a referenced direction  $s_x$ .

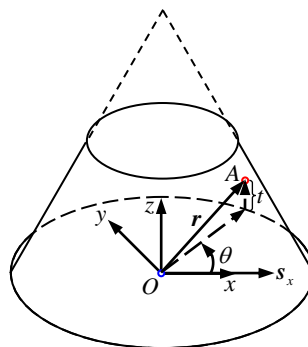


**Fig. 3** A conical surface.

Thus, if we set fixed reference frames in Figs. 1-3, which have points  $O$  as the origins, the  $x$ -axes along the directions of  $s_x$ , and the  $z$ -axes perpendicular to the circular surface and the bottoms of the cylinder and the conic, the expressions of these three basic kinds of quadrics can all be written as the following form,

$$\begin{cases} x = f_x(t, \theta) \\ y = f_y(t, \theta) \\ z = f_z(t, \theta) \end{cases} \quad (1)$$

### 3. Motion generators of quadrics

Based upon the analysis of the characteristics of the circular, cylindrical, and conical surfaces in Section 2, the mechanical structures that can generate these quadrics will be investigated in this section. These structures are called motion generators of quadrics. Here, we use finite screw as the mathematical tool to describe mechanical motion.

#### 3.1 Motion sets of one-DoF joints

As discussed in the authors' previous works [15, 23, 24], the motions generated by a revolute (R) joint, a prismatic (P) joint and a helical (H) joint can be described by sets of finite screws,

$$\{\mathbf{R}(P_R, s_R)\} = \left\{ 2 \tan \frac{\theta_R}{2} \begin{pmatrix} s_R \\ \mathbf{r}_{P_R} \times s_R \end{pmatrix} \middle| \theta_R \in [0, 2\pi] \right\}, \quad (2)$$

where  $\{\mathbf{R}(P_R, s_R)\}$  denotes the set of motions generated by an R joint with unit direction  $s_R$ , whose axis passes through point  $P_R$ ,  $\mathbf{r}_{P_R}$  is the position vector of point  $P_R$  that points from the origin of the fixed reference frame to that point,  $\theta_R$  is the rotational angle of the R joint measured from its initial pose;

$$\{\mathbf{T}(s_P)\} = \left\{ t_P \begin{pmatrix} \mathbf{0} \\ s_P \end{pmatrix} \middle| t_P \in \mathbb{R} \right\}, \quad (3)$$

where  $\{\mathbf{T}(s_P)\}$  denotes the motion set generated by a P joint with unit direction  $s_P$ ,  $t_P$  is the translational distance of the P joint with respect to its initial pose;

$$\{\mathbf{H}(P_H, s_H, h)\} = \left\{ 2 \tan \frac{\theta_H}{2} \begin{pmatrix} s_H \\ \mathbf{r}_{P_H} \times s_H \end{pmatrix} + h \theta_H \begin{pmatrix} \mathbf{0} \\ s_H \end{pmatrix} \middle| \theta_H \in [0, 2\pi] \right\}, \quad (4)$$

where  $\{\mathbf{H}(P_H, s_H, h)\}$  denotes the motion set generated by an H joint, whose axis has unit direction  $s_H$  and passes through point  $P_H$ ,  $\mathbf{r}_{P_H}$  is the position vector of point  $P_H$ ,  $\theta_H$  is the rotational angle of the H joint from its initial pose,  $h$  is its pitch.

#### 3.2 Motions generated by $R_a P_b R_a$ kinematic chain

Having the sets of finite screws generated by these one-DoF joints at hand, the motions generated by any serial kinematic chains can be expressed by using screw triangle product [24], which is the composition product of finite screws. We firstly investigate the motions of a  $R_a P_b R_a$  kinematic chain. Here-in-after, the subscript of a joint indicates its direction. This means that the unit direction vectors of joints  $R_a$  and  $P_b$  are  $s_a$  and  $s_b$ , respectively. The motion set generated by  $R_a P_b R_a$  is expressed as

$$\{\mathbf{M}_{R_a P_b R_a}\} = \{\mathbf{R}(A, s_a) \Delta \mathbf{T}(s_b) \Delta \mathbf{R}(O, s_a)\}, \quad (5)$$

where the axes of the two R joints respectively pass through points  $O$  and  $A$ . The expression of each factor in Eq. (5) can be given using Eqs. (2) and (3), as

$$\{\mathbf{R}(O, s_a)\} = \left\{ 2 \tan \frac{\theta_{a,1}}{2} \begin{pmatrix} s_a \\ \mathbf{r}_O \times s_a \end{pmatrix} \middle| \theta_{a,1} \in [0, 2\pi] \right\}, \quad (6)$$

$$\{\mathbf{R}(A, s_a)\} = \left\{ 2 \tan \frac{\theta_{a,2}}{2} \begin{pmatrix} s_a \\ \mathbf{r}_A \times s_a \end{pmatrix} \middle| \theta_{a,2} \in [0, 2\pi] \right\}, \quad (7)$$

$$\{T(s_b)\} = \left\{ t_b \begin{pmatrix} \mathbf{0} \\ s_b \end{pmatrix} \middle| t_b \in \mathbb{R} \right\}, \quad (8)$$

where the denotations of  $r_O$ ,  $r_A$ ,  $\theta_{a,1}$ ,  $\theta_{a,2}$ , and  $t_b$  can be referred to those of the symbols in Eqs. (2) and (3).

Using the computation properties of screw triangle product, the finite screw set of  $R_a P_b R_a$  can be rewritten in the following way

$$\begin{aligned} \{M_{R_a P_b R_a}\} &= \left\{ R(A, s_a) \Delta R(O, s_a) \Delta T(\exp(\theta_{a,1} [s_a \times]) s_b) \right\} \\ &= \left\{ 2 \tan \frac{\theta_{a,1} + \theta_{a,2}}{2} \begin{pmatrix} s_a \\ r_A \times s_a \end{pmatrix} \Delta \begin{pmatrix} \mathbf{0} \\ (\exp(\theta_{a,1} [s_a \times]) - E_3)(r_A - r_O) \end{pmatrix} \Delta t_b \begin{pmatrix} \mathbf{0} \\ \exp(\theta_{a,1} [s_a \times]) s_b \end{pmatrix} \right\}, \\ &= \left\{ 2 \tan \frac{\theta_{a,1} + \theta_{a,2}}{2} \begin{pmatrix} s_a \\ r_A \times s_a \end{pmatrix} \Delta \begin{pmatrix} \mathbf{0} \\ \exp(\theta_{a,1} [s_a \times]) (r_{A'} - r_{O'} + t_b s_b) - (r_{A'} - r_{O'}) \end{pmatrix} \right\} \end{aligned} \quad (9)$$

where  $[s_a \times]$  is the skew-symmetric matrix of the unit vector  $s_a$ ,  $r_{A'}$  and  $r_{O'}$  are the position vectors of the two R joint axes which are respectively perpendicular to the corresponding axes,

$$r_{O'} = r_O - (r_O^T s_a) s_a, \quad r_{A'} = r_A - (r_A^T s_a) s_a. \quad (10)$$

It can be clearly seen from Eq. (9) that the motions generated by  $R_a P_b R_a$  consist of two parts. One is rotational part, and the other is translational part. Hence, the translations of  $R_a P_b R_a$  can be obtained as

$$\{M_{R_a P_b R_a}\}^t = \left\{ \begin{pmatrix} \mathbf{0} \\ \exp(\theta_{a,1} [s_a \times]) (r_{A'} - r_{O'} + t_b s_b) - (r_{A'} - r_{O'}) \end{pmatrix} \right\}, \quad (11)$$

where the superscript of  $\{M_{R_a P_b R_a}\}^t$  indicates that it is the translational part of  $\{M_{R_a P_b R_a}\}$ .

For a given structure of  $R_a P_b R_a$ ,  $s_a$ ,  $s_b$ ,  $r_{A'}$  and  $r_{O'}$  are all known vectors, only  $\theta_{a,1}$  and  $t_b$  are the parameters in Eq. (11). Thus, Eq. (11) is an expression of two-DoF translations on quadrics.

### 3.3 Motion generators of different quadrics

When the direction vectors of  $R_a$  and  $P_b$  have different geometric relationships, the translations in Eq. (11) are on different quadrics. In other words,  $R_a P_b R_a$  with different conditions between  $s_a$  and  $s_b$  are the motion generators of different quadrics. In the following, we will investigate these motion generators of different quadrics in three cases.

(1) Motion generators of circular surfaces ( $s_a^T s_b = 0$ )

When the directions of  $R_a$  and  $P_b$  are perpendicular to each other, as shown in Fig. 4, Eq. (11) can be rewritten into the following form with considering the structure interference

$$\{M_{Ci}\} = \left\{ \begin{pmatrix} \mathbf{0} \\ \exp(\theta_{a,1} [s_a \times]) t'_b s_b - (r_{A'} - r_{O'}) \end{pmatrix} \middle| \theta_{a,1} \in [0, 2\pi], t'_b \in [-|r_{A'} - r_{O'}|, -2r_{R_a}] \right\}, \quad (12)$$

where  $\{M_{Ci}\}$  denotes the translations on a circular surface,  $r_{R_a}$  is the radius of the  $R_a$  joints, and

$$t'_b = t_b - |r_{A'} - r_{O'}|. \quad (13)$$

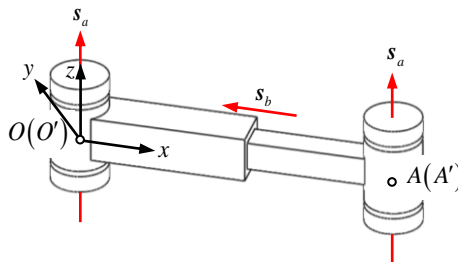


Fig. 4 Motion generator of circular surface.

$(\mathbf{r}_{A'} - \mathbf{r}_{O'})$  in Eq. (12) is the initial position of point  $A'$  with respect to point  $O'$ . Setting the opposite direction of  $\mathbf{s}_b$  as  $\mathbf{s}_x$  in Fig. 1, the parameters to identify any position of point  $A'$  on the circular surface are expressed as

$$\mathbf{r} = \exp(\theta_{a,1} [\mathbf{s}_a \times]) \mathbf{t}'_b \mathbf{s}_b, \quad \theta = \theta_{a,1}, \quad t = t'_b \quad (14)$$

Similar with Fig. 1, we set a fixed reference frame at point  $O'$ . In this way, the expression of the circular surface generated by the  $R_a P_b R_a$  kinematic chain in Fig. 4 is formulated as

$$\begin{cases} x = -t'_b \cos \theta_{a,1} \\ y = -t'_b \sin \theta_{a,1} \\ z = 0 \end{cases} \quad (15)$$

A group of values for the dimensions of this  $R_a P_b R_a$  kinematic chain is given in Table 1.

**Table 1** Dimensions of  $R_a P_b R_a$  kinematic chain with condition  $\mathbf{s}_a^T \mathbf{s}_b = 0$ .

$\mathbf{s}_a$	$\mathbf{s}_b$	$\mathbf{r}_{O'}$	$\mathbf{r}_{A'}$	$r_{R_a}$
(0;0;1)	(-1;0;0)	(0;0;0)	(3;0;0)	0.3

Using MATLAB® software and the values in Table 1, the circular surface generated by this  $R_a P_b R_a$  is drawn in Fig. 5, which verifies the above analysis.

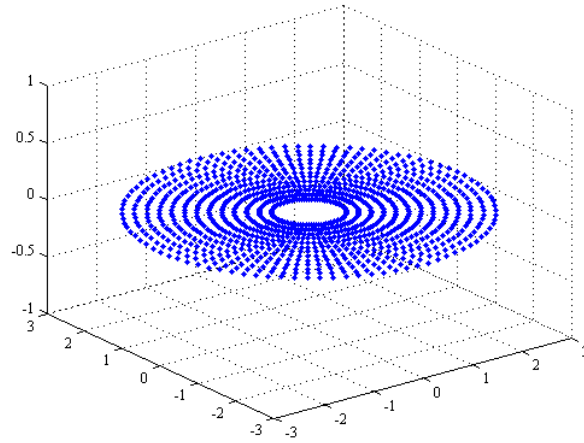


**Fig. 5** Circular surface generated by  $R_a P_b R_a$  with condition  $\mathbf{s}_a^T \mathbf{s}_b = 0$ .

According to the properties of screw triangle product, it can be easily proved that both the kinematic chains  $P_b R_a R_a$  and  $R_a R_a P_b$  with condition  $\mathbf{s}_a^T \mathbf{s}_b = 0$  as well as  $R_a R_a R_a$  generate the same one-DoF rotational and two-DoF translational motion pattern with  $R_a P_b R_a$ . Hence, these four serial kinematic chains are all motion generators of circular surfaces, as listed in Table 2.

**Table 2** Motion generators of circular surfaces.

No.	Kinematic chain	Equivalent motion pattern regardless of dimensions
1	$R_a P_b R_a (\mathbf{s}_a^T \mathbf{s}_b = 0)$	$\{\mathbf{R}(A, \mathbf{s}_a) \Delta \mathbf{T}(\mathbf{s}_b) \Delta \mathbf{R}(O, \mathbf{s}_a)\}$
2	$P_b R_a R_a (\mathbf{s}_a^T \mathbf{s}_b = 0)$	$\{\mathbf{R}(A, \mathbf{s}_a) \Delta \mathbf{R}(O, \mathbf{s}_a) \Delta \mathbf{T}(\mathbf{s}_b)\}$
3	$R_a R_a P_b (\mathbf{s}_a^T \mathbf{s}_b = 0)$	$\{\mathbf{T}(\mathbf{s}_b) \Delta \mathbf{R}(A, \mathbf{s}_a) \Delta \mathbf{R}(O, \mathbf{s}_a)\}$
4	$R_a R_a R_a$	$\{\mathbf{R}(A, \mathbf{s}_a) \Delta \mathbf{R}(B, \mathbf{s}_a) \Delta \mathbf{R}(O, \mathbf{s}_a)\}$

(2) Motion generators of cylindrical surfaces ( $|\mathbf{s}_a^T \mathbf{s}_b| = 1$ )

When  $R_a$  and  $P_b$  have parallel directions, it can be known that  $\mathbf{s}_b = \pm \mathbf{s}_a$ . As shown in Fig. 6, we discuss the situation that  $\mathbf{s}_b = \mathbf{s}_a$ . Thus, we can rewrite Eq. (11) as

$$\{\mathbf{M}_{Cy}\} = \left\{ \begin{pmatrix} \mathbf{0} \\ \exp(\theta_{a,1} [\mathbf{s}_a \times]) (\mathbf{r}_{A'} - \mathbf{r}_{O'} + t_b \mathbf{s}_a) - (\mathbf{r}_{A'} - \mathbf{r}_{O'}) \end{pmatrix} \middle| \theta_{a,1} \in [0, 2\pi], t_b \in [0, h] \right\}, \quad (16)$$

where  $\{\mathbf{M}_{Cy}\}$  denotes the translations on a cylindrical surface,  $h$  is the height of the corresponding cylinder.

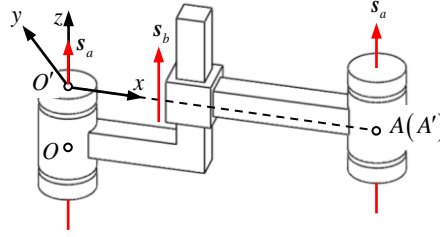


**Fig. 6** Motion generator of cylindrical surface.

In the translation vector of Eq. (16),  $(\mathbf{r}_{A'} - \mathbf{r}_{O'})$  is the initial position of point  $A'$  with respect to point  $O'$ . If we set the direction of  $(\mathbf{r}_{A'} - \mathbf{r}_{O'})$  as  $\mathbf{s}_x$  in Fig. 2, the parameters to identify any position of point  $A'$  on the cylindrical surface can be expressed as

$$\mathbf{r} = \exp(\theta_{a,1} [\mathbf{s}_a \times]) (\mathbf{r}_{A'} - \mathbf{r}_{O'} + t_b \mathbf{s}_a), \quad \theta = \theta_{a,1}, \quad t = t_b. \quad (17)$$

A fixed reference frame is set at point  $O'$  in the similar way with the reference frame in Fig. 2. Then, we can formulate the expression of the cylindrical surface generated by the  $R_a P_b R_a$  kinematic chain in Fig. 6 as

$$\begin{cases} x = |\mathbf{r}_{A'} - \mathbf{r}_{O'}| \cos \theta_{a,1} \\ y = |\mathbf{r}_{A'} - \mathbf{r}_{O'}| \sin \theta_{a,1} \\ z = t_b \end{cases} \quad (18)$$

In order to verify the above analysis, we use MATLAB<sup>®</sup> software and a group of values listed in Table 3 for the dimensions of this  $R_a P_b R_a$  kinematic chain to draw the cylindrical surface generated by the  $R_a P_b R_a$ , the result is shown in Fig. 7.

**Table 3** Dimensions of  $R_a P_b R_a$  kinematic chain with condition  $s_b = s_a$ .

$s_a$	$s_b$	$\mathbf{r}_{O'}$	$\mathbf{r}_{A'}$	$h$
(0;0;1)	(0;0;1)	(0;0;0)	(3;0;0)	1.5

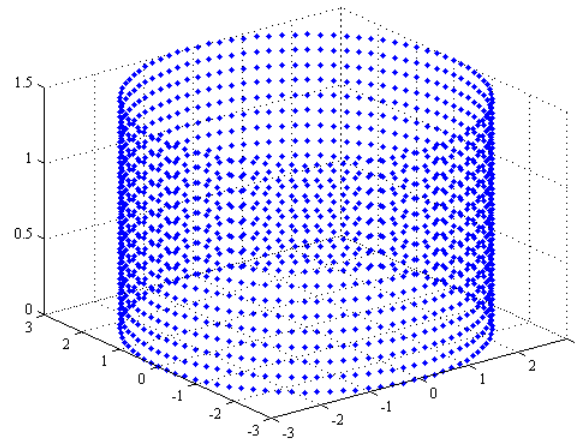


**Fig. 7** Cylindrical surface generated by  $R_a P_b R_a$  with condition  $s_b = s_a$ .

We can write  $R_a P_b R_a (s_b = s_a)$  as  $R_a P_a R_a$ . The movement of its  $P_a$  joint does not change the perpendicular distance between the axes of the two  $R_a$  joints. Thus, if we adjust the sequence of the  $P_a$  joint in the kinematic chain but maintain the perpendicular distance between the  $R_a$  joints' axes, the motions generated by the kinematic chain will not be

changed. It means that both the kinematic chains  $P_a R_a R_a$  and  $R_a R_a P_a$  generate the same motion pattern with  $R_a P_a R_a$ . In other words, these three serial kinematic chains are all motion generators of cylindrical surfaces.

Furthermore, when we replace one or two  $R_a$  joints in these kinematic chains by  $H_a$  joint(s), the translations of the  $H_a$  joint(s) can be offset by the  $P_a$  joint. Hence, the kinematic chains obtained through replacing  $R_a$  by  $H_a$  are also motion generators of cylindrical surfaces.

Totally, we can get twelve types of motion generators of cylindrical surfaces, as listed in Table 4. The equivalence among their motion patterns can be easily verified by using the properties of screw triangle product.

**Table 4** Motion generators of cylindrical surfaces.

No.	Kinematic chain	Equivalent motion pattern regardless of dimensions
1	$R_a P_a R_a$	$\{R(A, s_a) \Delta T(s_a) \Delta R(O, s_a)\}$
2	$P_a R_a R_a$	$\{R(A, s_a) \Delta R(O, s_a) \Delta T(s_a)\}$
3	$R_a R_a P_a$	$\{T(s_a) \Delta R(A, s_a) \Delta R(O, s_a)\}$
4	$H_a P_a R_a$	$\{R(A, s_a) \Delta T(s_a) \Delta H(O, s_a, h)\}$
5	$R_a P_a H_a$	$\{H(A, s_a, h) \Delta T(s_a) \Delta R(O, s_a)\}$
6	$H_a P_a H_a$	$\{H(A, s_a, h_2) \Delta T(s_a) \Delta H(O, s_a, h_1)\}$
7	$P_a H_a R_a$	$\{R(A, s_a) \Delta H(O, s_a, h) \Delta T(s_a)\}$
8	$P_a R_a H_a$	$\{H(A, s_a, h) \Delta R(O, s_a) \Delta T(s_a)\}$
9	$P_a H_a H_a$	$\{H(A, s_a, h_2) \Delta H(O, s_a, h_1) \Delta T(s_a)\}$
10	$H_a R_a P_a$	$\{T(s_a) \Delta R(A, s_a) \Delta H(O, s_a, h)\}$
11	$R_a H_a P_a$	$\{T(s_a) \Delta H(A, s_a, h) \Delta R(O, s_a)\}$
12	$H_a H_a P_a$	$\{T(s_a) \Delta H(A, s_a, h_2) \Delta H(O, s_a, h_1)\}$

### (3) Motion generators of conical surfaces ( $0 < |s_a^T s_b| < 1$ )

As shown in Fig. 8, if  $R_a$  and  $P_b$  have non-perpendicular and non-parallel directions, the geometric condition between them can be given as  $0 < |s_a^T s_b| < 1$ . In this case, Eq. (11) can be rewritten as

$$\{M_{Co}\} = \left\{ \begin{pmatrix} \mathbf{0} \\ \exp(\theta_{a,1} [s_a \times]) (r_{A'} - r_{O'} + t_b s_b) - (r_{A'} - r_{O'}) \end{pmatrix} \middle| \theta_{a,1} \in [0, 2\pi], t_b \in [0, l] \right\}, \quad (19)$$

where  $\{M_{Co}\}$  denotes the translations on a conical surface,  $l$  is the length along the conic generatrix from the bottom to the top.

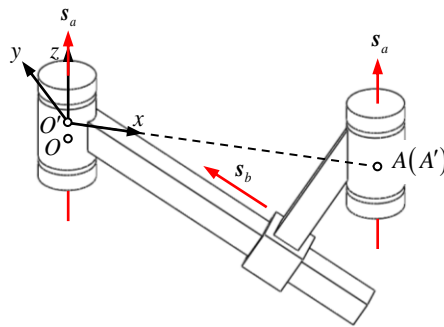


**Fig. 8** Motion generator of conical surface.

Similar with the above two cases,  $(r_{A'} - r_{O'})$  in the translation vector of Eq. (19) is the initial position of point  $A'$  with respect to point  $O'$ . If the direction of  $(r_{A'} - r_{O'})$  is set as  $s_x$  in Fig. 4, we can express the parameters to identify any position of point  $A'$  on the conical surface, as

$$r = \exp(\theta_{a,1} [s_a \times]) (r_{A'} - r_{O'} + t_b s_b), \quad \theta = \theta_{a,1}, \quad t = t_b \quad (20)$$

Set a fixed reference frame at point  $O'$  in the similar way with the reference frame in Fig. 4. In this fixed reference frame, the conical surface generated by the  $R_aP_bR_a$  kinematic chain in Fig. 8 is formulate as

$$\begin{cases} x = (|\mathbf{r}_{A'} - \mathbf{r}_{O'}| - |\mathbf{s}_b \times \mathbf{s}_a|) \cos \theta_{a,1} \\ y = (|\mathbf{r}_{A'} - \mathbf{r}_{O'}| - |\mathbf{s}_b \times \mathbf{s}_a|) \sin \theta_{a,1} \\ z = t_b \mathbf{s}_b^T \mathbf{s}_a \end{cases} \quad (21)$$

Using MATLAB® software and a group of values listed in Table 5 for the dimensions of this  $R_aP_bR_a$  kinematic chain, the conical surface generated by the  $R_aP_bR_a$  is drawn to verify the above analysis, as shown in Fig. 9.

**Table 5** Dimensions of  $R_aP_bR_a$  kinematic chain with condition  $\mathbf{s}_a^T \mathbf{s}_b = \sqrt{2}/2$ .

$\mathbf{s}_a$	$\mathbf{s}_b$	$\mathbf{r}_{O'}$	$\mathbf{r}_{A'}$	$l$
(0;0;1)	$(-\sqrt{2}/2; 0; \sqrt{2}/2)$	(0;0;0)	(3;0;0)	$1.5 \times \sqrt{2}$

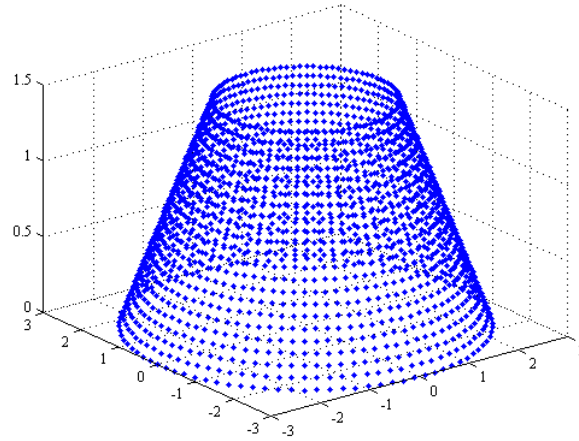


**Fig. 9** Conical surface generated by  $R_aP_bR_a$  with condition  $\mathbf{s}_a^T \mathbf{s}_b = \sqrt{2}/2$ .

Unlike  $R_aP_bR_a$  ( $\mathbf{s}_b = \mathbf{s}_a$ ), the movement of the  $P_b$  joint in  $R_aP_bR_a$  ( $0 < |\mathbf{s}_a^T \mathbf{s}_b| < 1$ ) will change the perpendicular distance between the two  $R_a$  joints' axes. After adjusting the sequence of the  $P_b$  joint in the kinematic chain, although this perpendicular distance will no longer be changed, the conical surface can still be generated, which means that both the kinematic chains  $P_bR_aR_a$  and  $R_aR_aP_a$  with condition of  $0 < |\mathbf{s}_a^T \mathbf{s}_b| < 1$  generate the same motion pattern with  $R_aP_aR_a$ . Thus, these three serial kinematic chains are all motion generators of conical surfaces, as listed in Table 6. It should be noted that replacing  $R_a$  by  $H_a$  of these kinematic chains will change their motion patterns.

**Table 6** Motion generators of conical surfaces.

No.	Kinematic chain	Equivalent motion pattern regardless of dimensions
1	$R_aP_bR_a$ ( $0 <  \mathbf{s}_a^T \mathbf{s}_b  < 1$ )	$\{\mathbf{R}(A, \mathbf{s}_a) \Delta \mathbf{T}(\mathbf{s}_b) \Delta \mathbf{R}(O, \mathbf{s}_a)\}$
2	$P_bR_aR_a$ ( $0 <  \mathbf{s}_a^T \mathbf{s}_b  < 1$ )	$\{\mathbf{R}(A, \mathbf{s}_a) \Delta \mathbf{R}(O, \mathbf{s}_a) \Delta \mathbf{T}(\mathbf{s}_b)\}$
3	$R_aR_aP_b$ ( $0 <  \mathbf{s}_a^T \mathbf{s}_b  < 1$ )	$\{\mathbf{T}(\mathbf{s}_b) \Delta \mathbf{R}(A, \mathbf{s}_a) \Delta \mathbf{R}(O, \mathbf{s}_a)\}$

Now, all the motion generators of circular, cylindrical, and conical surfaces have been synthesized.

#### 4. Closed-loop linkages to generate ellipse curves

In this section, a simple application of the motion generators of quadrics in the innovative design of closed-loop linkages will be discussed.

As is well known, the intersection curve of a cylindrical surface and a circular surface can be either a circle or an ellipse. In order to get an ellipse, the generatrix of the cylindrical surface and the normal of the circular surface should not be perpendicular or parallel to each other.

We try to use a motion generator of a cylindrical surface and that of a circular surface to constitute a closed-loop linkage which can generate ellipse curve. As shown in Fig. 10, a  $R_{1,a}P_{1,b}R_{1,a}$  ( $\mathbf{s}_{1,b} = \mathbf{s}_{1,a}$ ) and a  $R_{2,a}P_{2,b}R_{2,a}$  ( $\mathbf{s}_{2,a}^T \mathbf{s}_{2,b} = 0$ )



are utilized to constitute a linkage, which is denoted as  $R_{1,a}P_{1,a}R_{1,a}-R_{2,a}P_{2,b}R_{2,a}$ . Using Eqs. (5), (9), (16) and (12), the motions generated by  $R_{1,a}P_{1,a}R_{1,a}$  and  $R_{2,a}P_{2,b}R_{2,a}$  can be respectively expressed as

$$\begin{aligned} \{M_{R_{1,a}P_{1,a}R_{1,a}}\} &= \{R(A_1, s_{1,a}) \Delta T(s_{1,a}) \Delta R(O_1, s_{1,a})\} \\ &= \left\{ 2 \tan \frac{\theta_{1,a,1} + \theta_{1,a,2}}{2} \begin{pmatrix} s_{1,a} \\ \mathbf{r}_{A_1} \times s_{1,a} \end{pmatrix} \Delta \begin{pmatrix} \mathbf{0} \\ \exp(\theta_{1,a,1} [s_{1,a} \times]) (\mathbf{r}_{A_1'} - \mathbf{r}_{O_1'} + t_{1,b} s_{1,a}) - (\mathbf{r}_{A_1'} - \mathbf{r}_{O_1'}) \end{pmatrix} \right\}_{\substack{\theta_{1,a,1}, \theta_{1,a,2} \in [0, 2\pi], \\ t_{1,b} \in [0, h_1]}}, \quad (22) \end{aligned}$$

and

$$\begin{aligned} \{M_{R_{2,a}P_{2,b}R_{2,a}}\} &= \{R(A_2, s_{2,a}) \Delta T(s_{2,a}) \Delta R(O_2, s_{2,a})\} \\ &= \left\{ 2 \tan \frac{\theta_{2,a,1} + \theta_{2,a,2}}{2} \begin{pmatrix} s_{2,a} \\ \mathbf{r}_{A_2} \times s_{2,a} \end{pmatrix} \Delta \begin{pmatrix} \mathbf{0} \\ \exp(\theta_{2,a,1} [s_{2,a} \times]) t'_{2,b} s_{2,b} - (\mathbf{r}_{A_2'} - \mathbf{r}_{O_2'}) \end{pmatrix} \right\}_{\substack{\theta_{2,a,1}, \theta_{2,a,2} \in [0, 2\pi], \\ t'_{2,b} \in [-|\mathbf{r}_{A_2'} - \mathbf{r}_{O_2'}|, -2r_{R_{2,a}}]}}, \quad (23) \end{aligned}$$

where the denotations of the symbols in the above two equations can be referred to the corresponding ones in Eqs. (5), (9), (16) and (12).

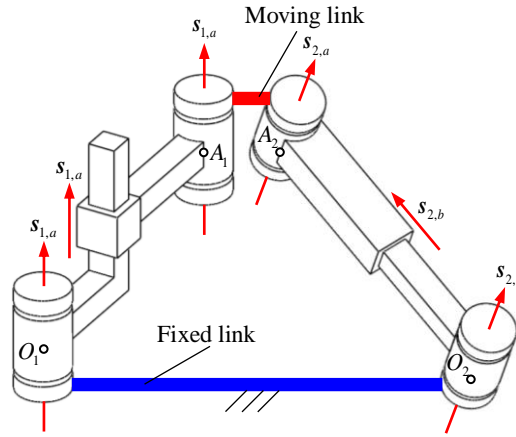


Fig. 10 Motion generator of ellipse curve.

According to the basic kinematic principle of mechanisms, the motions of the moving link of the linkage is the intersection of the motions generated by its two components, i.e.,  $R_{1,a}P_{1,a}R_{1,a}$  and  $R_{2,a}P_{2,b}R_{2,a}$ . Because the rotations generated by these two kinematic chains are about two different directions ( $s_{1,a}$  and  $s_{2,a}$ ), and have no intersection, the motions generated by the linkage are pure translations, which are obtained as

$$\begin{aligned} \{M_{R_{1,a}P_{1,a}R_{1,a}-R_{2,a}P_{2,b}R_{2,a}}\} &= \{M_{R_{1,a}P_{1,a}R_{1,a}}\} \cap \{M_{R_{2,a}P_{2,b}R_{2,a}}\} \\ &= \left\{ \begin{pmatrix} \mathbf{0} \\ \exp(\theta_{1,a,1} [s_{1,a} \times]) (\mathbf{r}_{A_1'} - \mathbf{r}_{O_1'} + t_{1,b} s_{1,a}) - (\mathbf{r}_{A_1'} - \mathbf{r}_{O_1'}) \end{pmatrix} \right\}_{\substack{\theta_{1,a,1} \in [0, 2\pi], \\ t_{1,b} \in [0, h_1]}} \\ &\cap \left\{ \begin{pmatrix} \mathbf{0} \\ \exp(\theta_{2,a,1} [s_{2,a} \times]) t'_{2,b} s_{2,b} - (\mathbf{r}_{A_2'} - \mathbf{r}_{O_2'}) \end{pmatrix} \right\}_{\substack{\theta_{2,a,1} \in [0, 2\pi], \\ t'_{2,b} \in [-|\mathbf{r}_{A_2'} - \mathbf{r}_{O_2'}|, -2r_{R_{2,a}}]}} \\ &= \{M_{Cy,1}\} \cap \{M_{Ci,2}\} \end{aligned} \quad (24)$$

where  $s_{1,a}$  is the direction of the generatrix of the cylindrical surface generated by  $R_{1,a}P_{1,a}R_{1,a}$ ,  $s_{2,a}$  is the direction of the normal of the circular surface generated by  $R_{2,a}P_{2,b}R_{2,a}$ .

In Fig. 10, it is easy to see that  $s_{1,a}$  and  $s_{2,a}$  are not perpendicular or parallel to each other, the relationship between them is  $0 < |s_{1,a}^T s_{2,a}| < 1$ . Hence, the intersection of the cylindrical surface generated by  $R_{1,a}P_{1,a}R_{1,a}$  and the circular surface generated by  $R_{2,a}P_{2,b}R_{2,a}$  is an ellipse curve. It means that the translations generated by the linkage in Fig. 10 are along an ellipse. In other words, the linkage is a motion generator of ellipse curve, as

$$\left\{ \mathbf{M}_{R_{1,a}P_{1,a}R_{1,a}-R_{2,a}P_{2,b}R_{2,a}} \right\} = \left\{ \mathbf{M}_{Cy,1} \right\} \cap \left\{ \mathbf{M}_{Ci,2} \right\}, \quad 0 < \left| \mathbf{s}_{1,a}^T \mathbf{s}_{2,a} \right| < 1 \quad (25)$$

$$= \left\{ \mathbf{M}_{El} \right\}$$

where  $\left\{ \mathbf{M}_{El} \right\}$  denotes the translations along an ellipse curve.

Using the kinematic chains in Tables 4 and 2, a few novel close-loop linkages can be invented, which generate ellipse curves. Besides  $R_{1,a}P_{1,a}R_{1,a}-R_{2,a}P_{2,b}R_{2,a}$ , other forty-seven linkages are synthesized. These motion generators of ellipse curves are listed in Table 7.

**Table 7** Motion generators of ellipse curves.

No.	Linkage	No.	Linkage	No.	Linkage	No.	Linkage
1	$R_{1,a}P_{1,a}R_{1,a}-R_{2,a}P_{2,b}R_{2,a}$	2	$R_{1,a}P_{1,a}R_{1,a}-P_{2,b}R_{2,a}R_{2,a}$	3	$R_{1,a}P_{1,a}R_{1,a}-R_{2,a}R_{2,a}P_{2,b}$	4	$R_{1,a}P_{1,a}R_{1,a}-H_{2,a}P_{2,b}R_{2,a}$
5	$R_{1,a}P_{1,a}R_{1,a}-R_{2,a}P_{2,b}H_{2,a}$	6	$R_{1,a}P_{1,a}R_{1,a}-H_{2,a}P_{2,b}H_{2,a}$	7	$R_{1,a}P_{1,a}R_{1,a}-P_{2,b}H_{2,a}R_{2,a}$	8	$R_{1,a}P_{1,a}R_{1,a}-P_{2,b}R_{2,a}H_{2,a}$
9	$R_{1,a}P_{1,a}R_{1,a}-P_{2,b}H_{2,a}H_{2,a}$	10	$R_{1,a}P_{1,a}R_{1,a}-H_{2,a}R_{2,a}P_{2,b}$	11	$R_{1,a}P_{1,a}R_{1,a}-R_{2,a}H_{2,a}P_{2,b}$	12	$R_{1,a}P_{1,a}R_{1,a}-H_{2,a}H_{2,a}P_{2,b}$
13	$P_{1,a}R_{1,a}R_{1,a}-R_{2,a}P_{2,b}R_{2,a}$	14	$P_{1,a}R_{1,a}R_{1,a}-P_{2,b}R_{2,a}R_{2,a}$	15	$P_{1,a}R_{1,a}R_{1,a}-R_{2,a}R_{2,a}P_{2,b}$	16	$P_{1,a}R_{1,a}R_{1,a}-H_{2,a}P_{2,b}R_{2,a}$
17	$P_{1,a}R_{1,a}R_{1,a}-R_{2,a}P_{2,b}H_{2,a}$	18	$P_{1,a}R_{1,a}R_{1,a}-H_{2,a}P_{2,b}H_{2,a}$	19	$P_{1,a}R_{1,a}R_{1,a}-P_{2,b}H_{2,a}R_{2,a}$	20	$P_{1,a}R_{1,a}R_{1,a}-P_{2,b}R_{2,a}H_{2,a}$
21	$P_{1,a}R_{1,a}R_{1,a}-P_{2,b}H_{2,a}H_{2,a}$	22	$P_{1,a}R_{1,a}R_{1,a}-H_{2,a}R_{2,a}P_{2,b}$	23	$P_{1,a}R_{1,a}R_{1,a}-R_{2,a}H_{2,a}P_{2,b}$	24	$P_{1,a}R_{1,a}R_{1,a}-H_{2,a}H_{2,a}P_{2,b}$
25	$R_{1,a}R_{1,a}P_{1,a}-R_{2,a}P_{2,b}R_{2,a}$	26	$R_{1,a}R_{1,a}P_{1,a}-P_{2,b}R_{2,a}R_{2,a}$	27	$R_{1,a}R_{1,a}P_{1,a}-R_{2,a}R_{2,a}P_{2,b}$	28	$R_{1,a}R_{1,a}P_{1,a}-H_{2,a}P_{2,b}R_{2,a}$
29	$R_{1,a}R_{1,a}P_{1,a}-R_{2,a}P_{2,b}H_{2,a}$	30	$R_{1,a}R_{1,a}P_{1,a}-H_{2,a}P_{2,b}H_{2,a}$	31	$R_{1,a}R_{1,a}P_{1,a}-P_{2,b}H_{2,a}R_{2,a}$	32	$R_{1,a}R_{1,a}P_{1,a}-P_{2,b}R_{2,a}H_{2,a}$
33	$R_{1,a}R_{1,a}P_{1,a}-P_{2,b}H_{2,a}H_{2,a}$	34	$R_{1,a}R_{1,a}P_{1,a}-H_{2,a}R_{2,a}P_{2,b}$	35	$R_{1,a}R_{1,a}P_{1,a}-R_{2,a}H_{2,a}P_{2,b}$	36	$R_{1,a}R_{1,a}P_{1,a}-H_{2,a}H_{2,a}P_{2,b}$
37	$R_{1,a}R_{1,a}R_{1,a}-R_{2,a}P_{2,b}R_{2,a}$	38	$R_{1,a}R_{1,a}R_{1,a}-P_{2,b}R_{2,a}R_{2,a}$	39	$R_{1,a}R_{1,a}R_{1,a}-R_{2,a}R_{2,a}P_{2,b}$	40	$R_{1,a}R_{1,a}R_{1,a}-H_{2,a}P_{2,b}R_{2,a}$
41	$R_{1,a}R_{1,a}R_{1,a}-R_{2,a}P_{2,b}H_{2,a}$	42	$R_{1,a}R_{1,a}R_{1,a}-H_{2,a}P_{2,b}H_{2,a}$	43	$R_{1,a}R_{1,a}R_{1,a}-P_{2,b}H_{2,a}R_{2,a}$	44	$R_{1,a}R_{1,a}R_{1,a}-P_{2,b}R_{2,a}H_{2,a}$
45	$R_{1,a}R_{1,a}R_{1,a}-P_{2,b}H_{2,a}H_{2,a}$	46	$R_{1,a}R_{1,a}R_{1,a}-H_{2,a}R_{2,a}P_{2,b}$	47	$R_{1,a}R_{1,a}R_{1,a}-R_{2,a}H_{2,a}P_{2,b}$	48	$R_{1,a}R_{1,a}R_{1,a}-H_{2,a}H_{2,a}P_{2,b}$

Noted:  $\mathbf{s}_{2,a}^T \mathbf{s}_{2,b} = 0$ ,  $0 < \left| \mathbf{s}_{1,a}^T \mathbf{s}_{2,a} \right| < 1$ .

Using the motion generators of quadrics studied in this paper, the closed-loop linkages which generate other kinds of conic sections (Apollonius conic sections) can also be synthesized. The details will be provided by the authors in a separate paper.

## 5. Conclusions

By using finite screw as mathematical tool, this paper studies some new mechanisms with new motion patterns. Mechanisms which generate translations on circular, cylindrical, and conical surfaces, as well as along ellipse curves, are presented. The following conclusions are drawn:

- (1) The translations on the three basic kinds of quadrics are expressed analytically, which will lead to the algebraic synthesis of their motion generators.
- (2) The motion generators of cylindrical and conical surfaces are synthesized in this paper for the first time, although the generators of circular surfaces have been reported in some existing works.
- (3) Having the motion generators of these quadrics at hand, the closed-loop linkages which purely generate one-DoF translations along ellipse curves as well as other conic sections (parabola curves and hyperbola curves) can be invented.

The theoretical research works in this paper introduce new motion patterns of serial kinematic chains and closed-loop linkages, and provide foundations for the innovative design of mechanisms and robots that can be applied in machining and manufacturing of complex surfaces and curves.

## Acknowledgments

This research work was supported by the research project of The Hong Kong Polytechnic University [Grant No. 1-45-37-ZE97]; and the National Natural Science Foundation of China (NSFC) [Grant Nos. 51575544 and 51875391].

## References

- [1] X.W. Kong, C.M. Gosselin, Type Synthesis of Parallel Mechanisms, Springer, Berlin, 2007.
- [2] Y. Qi, T. Sun, Y.M. Song, Type synthesis of parallel tracking mechanism with varied axes by modeling its finite motions algebraically, ASME Journal of Mechanisms and Robotics 9 (5) (2017) 054504-1-054504-6.
- [3] J. Meng, G.F. Liu, Z.X. Li, A geometric theory for analysis and synthesis of sub-6 DoF parallel manipulators, IEEE Transactions on Robotics 23 (4) (2007) 625-649.
- [4] L.W. Tsai, Robot Analysis: The Mechanics of Serial and Parallel Manipulators, John Wiley & Sons, Inc., New York, 1999.
- [5] X.M. Huo, T. Sun, Y.M. Song, et al., An analytical approach to determine motions/constraints of serial kinematic chains based on Clifford algebra, Proceedings of the Institution of Mechanical Engineers, Part C: Journal of Mechanical Engineering Science 231 (7) (2017) 1324-1338.
- [6] Y. Qi, T. Sun, Y.M. Song, Multi-objective optimization of parallel tracking mechanism considering parameter uncertainty, ASME Journal of Mechanisms and Robotics 10 (4) (2018) 041006-1-041006-12.

- [7] X.J. Liu, X. Chen, M. Nahon, Motion/force constrainability analysis of lower-mobility parallel manipulators, *ASME Journal of Mechanisms and Robotics* 6 (3) (2014) 031006-1-031006-9.
- [8] T. Sun, Y.M. Song, G. Dong, et al., Optimal design of a parallel mechanism with three rotational degrees of freedom, *Robotics and Computer-Integrated Manufacturing* 28 (4) (2012) 500-508.
- [9] P.C. López-Custodio, A. Müller, J.M. Rico, et al., A synthesis method for 1-DOF mechanisms with a cusp in the configuration space, *Mechanism and Machine Theory* 132 (2019) 154-175.
- [10] G.W. Wei, J.S. Dai, A spatial eight-bar linkage and its association with the deployable platonic mechanisms, *ASME Journal of Mechanisms and Robotics* 6(2) (2014) 021010-1-021010-9.
- [11] Y. Chen, Z. You, Spatial 6R linkages based on the combination of two Goldberg 5R linkages, *Mechanism and Machine Theory* 42 (11) (2007) 1484-1498.
- [12] H.J. Feng, Y. Chen, J.S. Dai, et al., Kinematic study of the general plane-symmetric Bricard linkage and its bifurcation variations, *Mechanism and Machine Theory* 116 (2017) 89-104.
- [13] Y. Chen, Z. You, On mobile assemblies of Bennett linkages, *Proceedings of the Royal Society A: Mathematical, Physical and Engineering Sciences* 464 (2003) (2008) 1275-1293.
- [14] J.M. Hervé, F. Sparacino, Structural synthesis of parallel robots generating spatial translation, In: *Proceedings of the 5th IEEE International Conference on Advanced Robotics*, 1991, pp. 808-813.
- [15] S.F. Yang, T. Sun, T. Huang, et al., A finite screw approach to type synthesis of three-DOF translational parallel mechanisms, *Mechanism and Machine Theory* 104 (2016) 405-419.
- [16] X.W. Kong, C.M. Gosselin, Type synthesis of 3-DOF translational parallel manipulators based on screw theory, *ASME Journal of Mechanical Design* 126 (1) (2004) 83-92.
- [17] Y. Qi, T. Sun, Y.M. Song, et al., Topology synthesis of three-legged spherical parallel manipulators employing Lie group theory, *Proceedings of the Institution of Mechanical Engineers, Part C: Journal of Mechanical Engineering Science* 229 (10) (2015) 1873-1886.
- [18] T. Sun, X.M. Huo, Type synthesis of 1T2R parallel mechanisms with parasitic motions, *Mechanism and Machine Theory* 128 (2018) 412-428.
- [19] Z.M. Bi, Y. Jin, Kinematic modeling of Exechon parallel kinematic machine, *Robotics and Computer-Integrated Manufacturing* 27 (1) (2011) 186-193.
- [20] Q.C. Li, J.M. Hervé, Type synthesis of 3-DOF RPR-equivalent parallel mechanisms, *IEEE Transactions on Robotics* 30 (6) (2014) 1333-1343.
- [21] X.W. Kong, C.M. Gosselin, Type synthesis of 3T1R 4-DOF parallel manipulators based on screw theory, *IEEE Transactions on Robotics and Automation* 20 (2) (2004) 181-190.
- [22] Q.C. Li, J.M. Hervé, Parallel mechanisms with bifurcation of Schoenflies motion, *IEEE Transactions on Robotics* 25 (1) (2009) 158-164.
- [23] S.F. Yang, T. Sun, T. Huang, Type synthesis of parallel mechanisms having 3T1R motion with variable rotational axis, *Mechanism and Machine Theory* 109 (2017) 220-230.
- [24] T. Sun, S.F. Yang, T. Huang, et al., A way of relating instantaneous and finite screws based on the screw triangle product, *Mechanism and Machine Theory* 108 (2017) 75-82.
- [25] J.S. Dai, *Geometrical Foundations and Screw Algebra for Mechanisms and Robotics*, Higher Education Press, Beijing, 2014. ISBN: 9787040334838 (translated from J.S. Dai, *Screw Algebra and Kinematic Approaches for Mechanisms and Robotics*, Springer, London, 2019.)
- [26] J.S. Dai, Finite displacement screw operators with embedded Chasles' motion, *ASME Journal of Mechanisms and Robotics* 4 (4) (2012) 041002-1-041002-9.
- [27] Y.M. Li, Q.S. Xu, Kinematic analysis of a 3-PRS parallel manipulator, *Robotics and Computer-Integrated Manufacturing* 23 (4) (2007) 395-408.
- [28] Y.M. Li, Q.S. Xu, Design and development of a medical parallel robot for cardiopulmonary resuscitation, *IEEE/ASME Transactions on Mechatronics* 12 (3) (2007) 265-273.
- [29] T. Sun, Y.P. Zhai, Y.M. Song, et al., Kinematic calibration of a 3-DoF rotational parallel manipulator using laser tracker, *Robotics and Computer-Integrated Manufacturing* 41 (2016) 78-91.
- [30] B.B. Lian, T. Sun, Y.M. Song, Parameter sensitivity analysis of a 5-DoF parallel manipulator, *Robotics and Computer-Integrated Manufacturing* 46 (2017) 1-14.
- [31] T. Sun, D. Liang, Y.M. Song, Singular-perturbation-based nonlinear hybrid control of redundant parallel robot, *IEEE Transactions on Industrial Electronics* 65 (4) (2018) 3326-3336.
- [32] D. Liang, Y.M. Song, T. Sun, Nonlinear dynamic modeling and performance analysis of a redundantly actuated parallel manipulator with multiple actuation modes based on FMD theory, *Nonlinear Dynamics* 89 (1) (2017) 391-428.
- [33] Y.M. Li, Q.S. Xu, Dynamic modeling and robust control of a 3-PRC translational parallel kinematic machine, *Robotics and Computer-Integrated Manufacturing* 25 (3) (2009) 630-640.
- [34] Y.M. Li, Y.G. Liu, X.P. Liu, et al., Parameter identification and vibration control in modular manipulators, *IEEE/ASME Transactions on Mechatronics* 9 (4) (2004) 700-705.
- [35] T. Sun, B.B. Lian, Stiffness and mass optimization of parallel kinematic machine, *Mechanism and Machine Theory* 120 (2018) 73-88.
- [36] T. Sun, H. Wu, B.B. Lian, et al., Stiffness modeling, analysis and evaluation of a 5 degree of freedom hybrid manipulator for friction stir welding, *Proceedings of the Institution of Mechanical Engineers, Part C: Journal of Mechanical Engineering Science* 231 (23) (2017) 4441-4456.
- [37] T. Sun, B.B. Lian, Y.M. Song, Stiffness analysis of a 2-DoF over-constrained RPM with an articulated traveling platform, *Mechanism and Machine Theory* 96 (2016) 165-178.
- [38] B.B. Lian, T. Sun, Y.M. Song, et al., Stiffness analysis and experiment of a novel 5-DoF parallel kinematic machine considering gravitational effects, *International Journal of Machine Tools and Manufacture* 95 (2015) 82-96.